



INTERNATIONAL ATOMIC ENERGY AGENCY
UNITED NATIONS EDUCATIONAL SCIENTIFIC AND CULTURAL ORGANIZATION



INTERNATIONAL CENTRE FOR THEORETICAL PHYSICS
34100 TRIESTE (ITALY) - P.O.B. 506 - MIRAMARE - STRADA COSTIERA 11 - TELEPHONES: 224-281/284/658
CABLE: CENTRATON - TELEX 460392-1

SMR/115 - 8

WINTER COLLEGE ON LASERS, ATOMIC AND MOLECULAR PHYSICS

(21 January - 22 March 1985)

STATISTICAL PROPERTIES OF OPTICAL FIELDS EXPERIMENTS

V. DEGIORGIO
Istituto di Fisica Applicata
Via Bassi, 6
27100 Pavia
Italy

These are preliminary lecture notes, intended only for distribution to participants.
Missing or extra copies are available from Room 229.

STATISTICAL PROPERTIES OF OPTICAL FIELDS

EXPERIMENTS

$W_1(E)$

probability density for the field complex amplitude

$$\rightarrow p(n) \rightarrow p(m)$$

probability distributions for photon number n or photoelectron number m

$W_2(E(t), E(t+\tau))$

joint probability density

$$p_2(n_1(t), n_2(t)) \rightarrow p_2(m_1, m_2)$$

joint photon (or photon count) distributions

\vdots
 W_m

$$G_2 = \langle E^{(1)}(t) E^{(2)}(t+\tau) E^{(3)}(t+\tau) E^{(4)}(t) \rangle$$

second-order field correlation function

$$\langle n_1(t) n_2(t+\tau) \rangle$$

photon number correlation function

The connection between the two columns is given by:

$$p(n) = \int d^2E W_1(E) \frac{(pT|E|^2)^n}{n!} e^{-pT|E|^2}$$

where p = experimental constant

T = measuring interval for the photon number n

Furthermore:

$$p(n) = \sum p(n) \underbrace{\binom{n}{m}}_{\text{Bernoulli}} \gamma^m (1-\gamma)^{n-m}$$

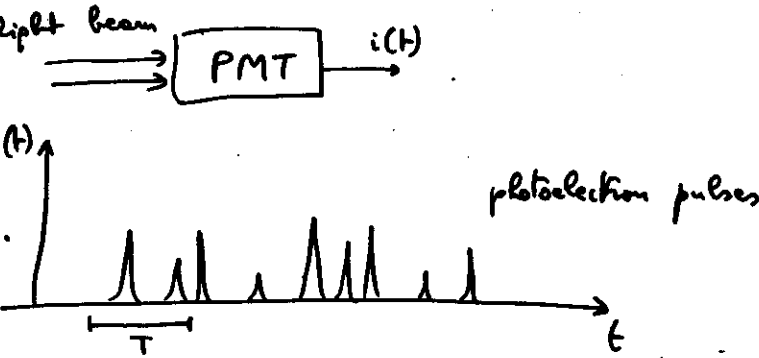
$$\langle m \rangle = \gamma \langle n \rangle \quad \gamma: \text{efficiency of the detector}$$

(3)

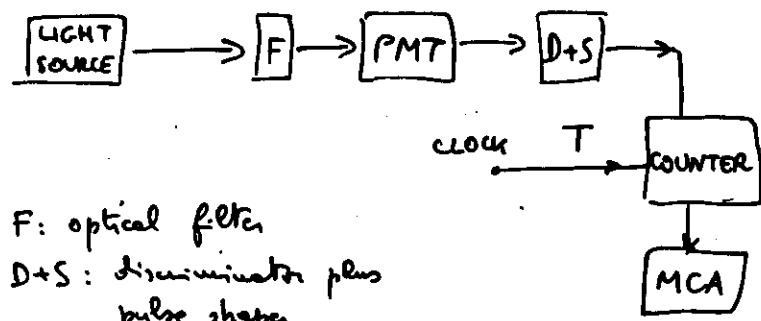
Detectors of e.m. waves at optical frequencies work through the absorption of e.m. energy in quantized steps (absorption of photons) and the consequent excitation (or emission) of electrons.

Photon counting techniques rely on a photoelectric detector, the photomultiplier tube (PMT), which is able to give at the output a measurable electric pulse after the absorption of a single photon.

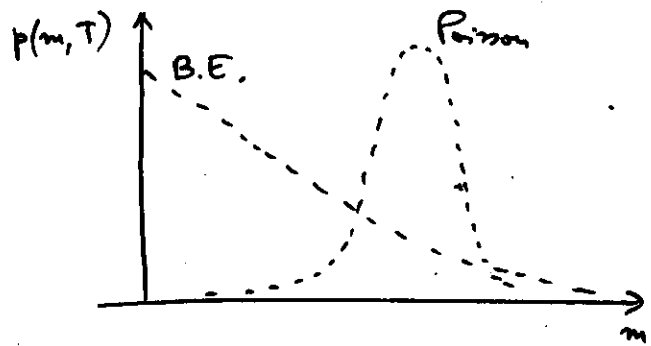
If the optical signal is so weak that it is very unlikely to detect more than one photon within the response time of the photodetector, the output electric current consists of a random train of nonoverlapping photoelectron pulses.



Photoelectron pulses are not identical because the PMT is a statistical device. The experimental apparatus includes a discriminator (to eliminate small spurious pulses) and a standardizer (to present pulses of standard shape to the counter). The output of the counter is sent to a multichannel analyzer (MCA).



F: optical filter
 D+S: discriminator plus
 pulse shaper



Experimental problems:

- how long should be T ?

$$\tau_d \ll T \ll \tau_{c2}$$

- how long should be the sampling interval T_s ?

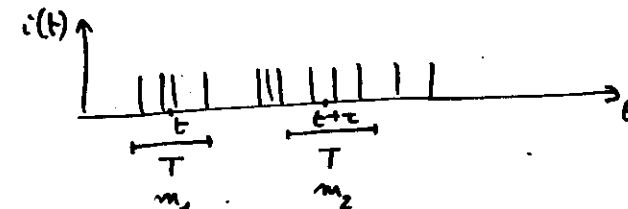
$$T_s > \tau_{c2}$$

- dead-time effect

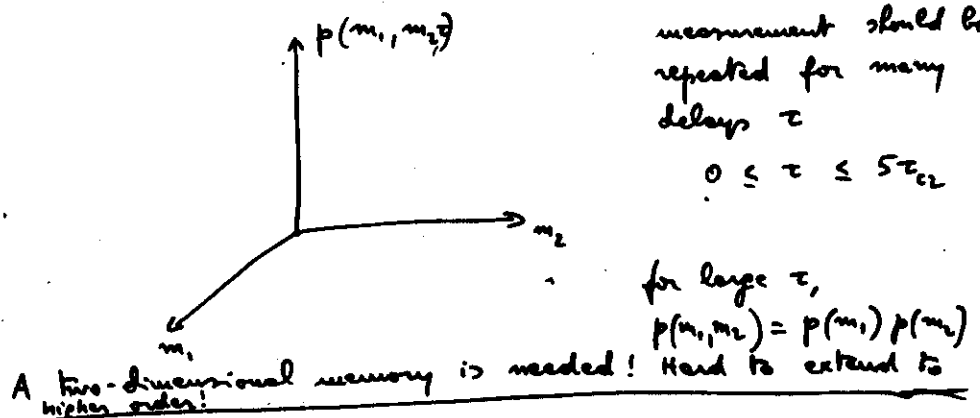
- noise (uncorrelated) — electronic
optical

τ_{c2} is the correlation time for intensity fluctuations

Joint photocount distributions



$T \ll \tau_{c2}$,
 measurement should be
 repeated for many
 delays τ
 $0 \leq \tau \leq 5\tau_{c2}$



A two-dimensional memory is needed! Hard to extend to higher order.

Two important cases :

ideal laser field $p(n) = \frac{\langle n \rangle^n}{n!} e^{-\langle n \rangle}$ Poisson

chaotic source(single-mode) $p(n) = \frac{\langle n \rangle^n}{(1+\langle n \rangle)^{n+1}}$ Bose-Einstein

Note that $p(n)$ remains Poisson or Bose-Einstein with $\langle m \rangle = \gamma \langle n \rangle$. In general, $p(n)$ is different from $p(n)$!

Beam through a mirror

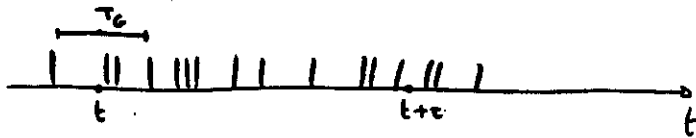
$$\xrightarrow{R} | \xrightarrow{R}$$

$$p(n) = p(n) * \text{Bernoulli} \text{ (with } \gamma = 1-R)$$

Cohesive state remains a cohesive state, n -state would change to a Bernoulli $p(n)$.

Digital correlators

The signal coming from the PMT is already in digital form



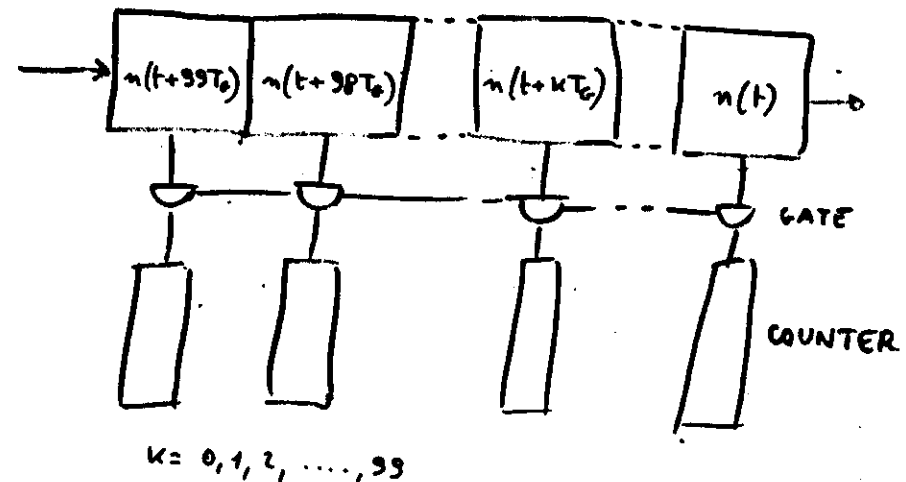
$n(t, T_G)$ is the number of photoelectron pulses counted in an interval T_G centered around time t . The autocorrelation function of the random variable n is

$$R(\tau, T_G) = \langle n(t, T_G) n(t+\tau, T_G) \rangle$$

If $T_G \ll \tau_c$, decay time of $G_2(\tau)$, then

$$R(\tau, T_G) \propto G_2(\tau)$$

The maximum number of photoelectron pulses n recorded in the interval T_G is limited by the deadtime of the apparatus. If real time operation is desired at high sampling frequencies, another limit is set by the fact that large numbers require long multiplication and registration times.



$n(t)$ before being kicked out by the sample $n(t+100T_G)$ is multiplied by all the 99 samples $n(t+kT_G)$. The result of each multiplication is stored into the appropriate counter. Present state of the art : 4 bits, 20 MHz.

In the low frequency range it is possible to build "software correlators", which feed directly into a computer without intermediate hardware.

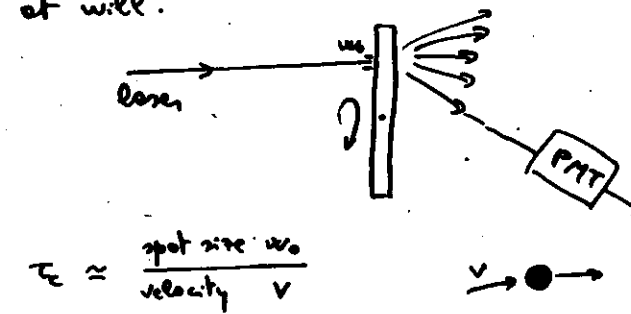
The technique can be extended to higher order intensity correlations $G_n(x_1, \dots, x_n; z_1, \dots, z_n)$

In some cases it is possible to measure G_n directly by using multiphoton absorption or harmonic generation (picosecond pulses, see later)

Chaotic source : any conventional lamp

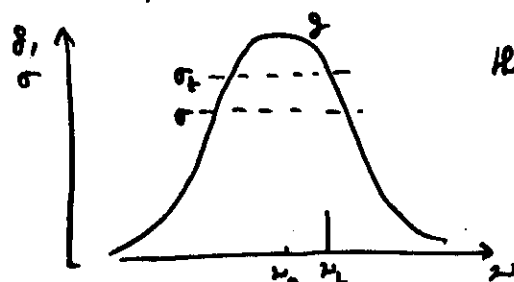
It is possible to measure the correlation functions $G_1(\tau)$ and $G_2(\tau)$. In particular the measurement of G_2 by Hershberg-Brown and Twiss around 1955 marks the beginning of quantum optics.

It is very difficult to measure $\rho(m)$ because $\tau_c \approx 1 \text{ ns}$. However, one can make a chaotic source by using a coherent source (laser) plus a random scatterer (ground-glass disk in the first experiments). In this case, τ_c is determined by the velocity of the disk and can be controlled at will.



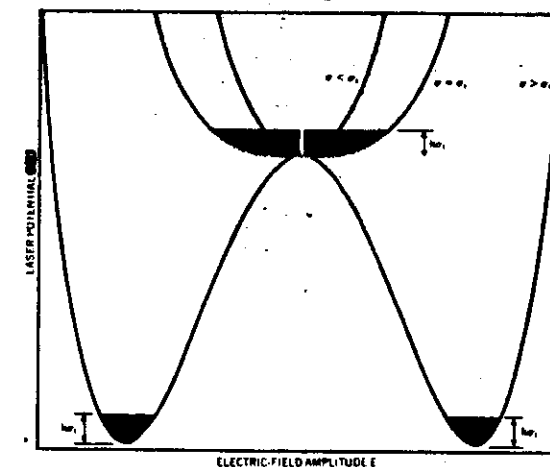
(Mikitinman-Spiller, Arechi and coworkers)

Laser - single-mode : is a coherent source well above threshold, but what happens in the threshold region?



7

FIGURES



The laser potential $V(E)$, the minima of which give the steady states of the laser. The three cases shown are: below threshold (unsaturated population inversion ν less than its threshold value ν_0), at threshold and above it. The magnitudes of the fluctuations of the laser field E at steady state are found by considering energy fluctuations δE , (see equation 4) above the minima of $V(E)$ and deriving the corresponding changes in the field amplitude.

FIGURE 1

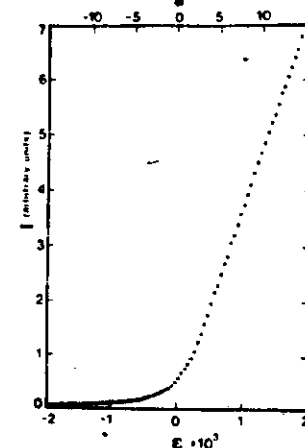
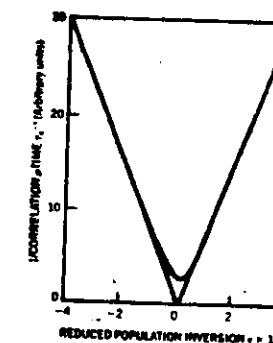


FIG. 2. The average laser intensity as a function of the normalized net gain (lower scale) and of the pump parameter n (upper scale). Errors are smaller than the dot size. The theoretical curve is not distinguishable from the line interpolating the experimental points.



The reciprocal of the correlation time τ_c of laser-intensity fluctuations plotted versus ν . Apart from the threshold region ($\nu = 0$), where rounding-off errors because of the finite laser volume, the correlation time follows a simple power law, which has an analog in the Landau-Ginzburg theory. The measurements are described in reference 10.

FIGURE 3

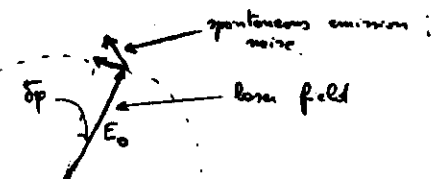


FIGURE 4

δp : phase shift due to single spontaneous emission event $\delta p = \frac{1}{E_0} = \frac{1}{P_{out}^{1/2}}$

Random walk : $\langle (\Delta p)^2 \rangle = N \langle \delta p^2 \rangle =$

$$+ \sigma t \frac{1}{P_{out}}$$

Cohesive time $\tau_c \rightarrow \langle \Delta p \rangle^2 \sim \sigma$

$$\tau_c \div \frac{P_{out}}{\sigma}$$

$$M_K = \sum n^k p(n)$$

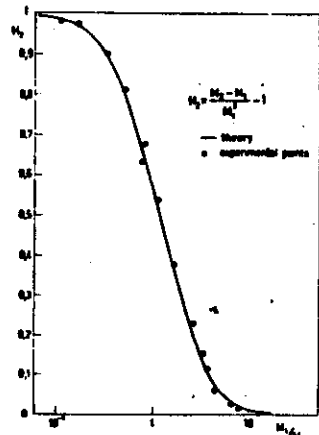


Fig. 17. The reduced second-order factorial moment H_2 as a function of the normalized laser intensity M_1/M_{10} . M_{10} denotes here the average intensity at threshold. The solid line represents theoretical values, the dots represent the experimental results (Arechi et al. 1967a).

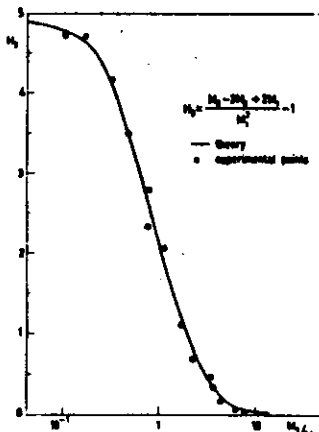
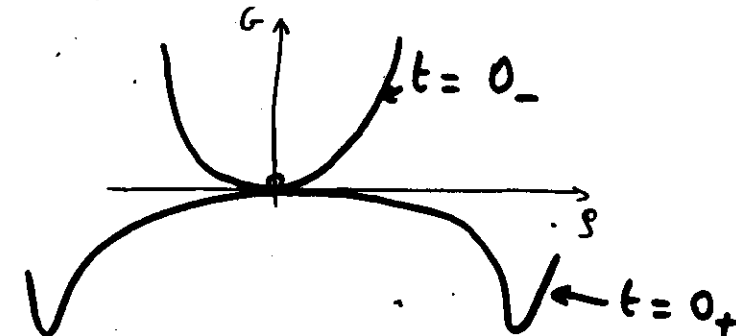


Fig. 18. Plot of H_2 versus M_1/M_{10} . Explanations are as for fig. 17.

Instability transients (Q-switching)

Fluctuations may be large even far away from threshold : decay of an unstable state characterized by the absence of systematic forces.



Decay initiated by a fluctuation

Linear amplification \rightarrow saturation \rightarrow steady state

Single-mode laser : Van der Pol equation

$$\dot{I} = \alpha I - 2\beta I^2$$

$$I = |E|^2, \quad \alpha = 2(\gamma_0 - \gamma)$$

Peak of the variance in correspondence with the inflection point of the average intensity transient
(Arechi, Degiorgio, Puercole Phys. Rev. Lett. 1967)

Phenomenological model (Arechi-Degiorgio Phys. Rev. 1971): deterministic evolution from a statistically defined initial condition.

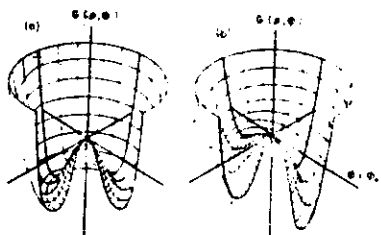


Fig. 5(a) Effective free energy, $G(p, q)$, of laser. (b) Effective free energy, $G(p, q)$, of laser subjected to symmetry-breaking signal having phase ϕ_0 .

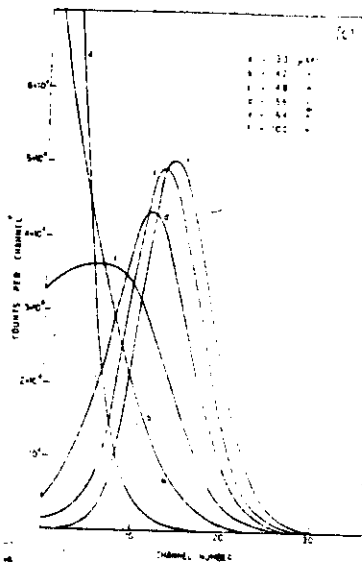


FIG. 6 Experimental statistical photocount distributions obtained with different delays with respect to the switching time. The solid lines join the experimental points which are not shown, to make the figure clearer. All distributions are normalized to the same area.

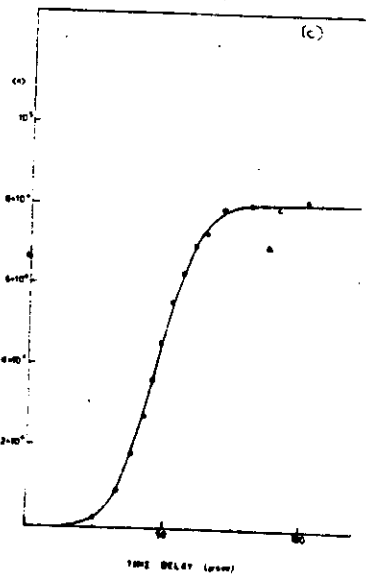


FIG. 7. Evolution of the average photon number ($\langle n \rangle$) inside the cavity as a function of the time delay τ . Solid line represents best-fit results computed from the theory of Brune, Lemoine, and Bergman.

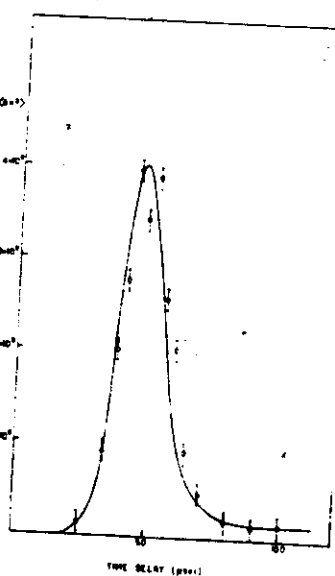
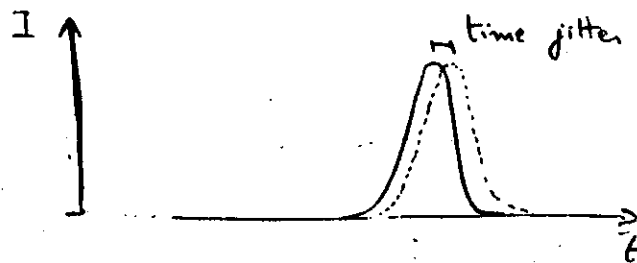


FIG. 8. Evolution of the variance $(\Delta n)^2$ of the statistical distribution of photons inside the cavity, as a function of the time delay. Solid lines represent theoretical results.



Q-switching pulse : fluctuations in shape and area are negligible (ideal laser), there is only a time jitter (fluctuation in time position) due to the initial statistics : number of photons which are present in the cavity at the Q-switching instant is a random variable with a Bose-Einstein distribution. Time jitter is comparable to pulse duration!

Conclusions about intrinsic noise :

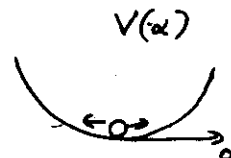
- c.w. single mode laser : for short threshold (normal operation) fluctuations are negligible
- pulsed laser : fluctuations only in the time position of the peak
- multimode laser : depends on mode interactions

External noise :

- pump fluctuations \rightarrow effect laser amplitude
- cavity length fluctuations \rightarrow effect laser frequency
- mirror parallelism fluctuations \rightarrow effect laser amplitude, may introduce transverse modes

Statistical theory of the single-mode laser

Recall damped harmonic oscillator
 $\ddot{\alpha} + \gamma \dot{\alpha} + \omega_0^2 \alpha = 0$



If damping constant $\gamma \ll \omega_0$,

$$\ddot{\alpha} + \gamma \dot{\alpha} = \Gamma(t) \quad \text{Langevin Eq.}$$

$\Gamma(t)$: complex stationary Gaussian process

$$\langle \Gamma(t) \rangle = 0; \langle \Gamma^*(t) \Gamma(t+\tau) \rangle = Q \delta(\tau)$$

α : Markov process, characterized fully by its conditional probability

$$W_c(\alpha_0, 0/\alpha, t)$$

From Langevin Eq. \rightarrow Fokker-Planck Eq. for W_c :

$$\frac{\partial W_c}{\partial t} - \gamma \operatorname{div}_\alpha (\alpha W_c) = \frac{Q}{4} \nabla_\alpha^2 W_c$$

$$\text{Solution: } W_c = \frac{1}{\pi \sigma^2(t)} \exp \left[- \frac{(\alpha - \alpha_0 e^{-\gamma t})^2}{\sigma^2(t)} \right]$$

$$\text{Gaussian (linear process)} \quad \sigma^2(t) = \frac{Q}{2\gamma} [1 - \exp(-2\gamma t)]$$

$$\lim_{t \rightarrow \infty} W_c = W_c(\alpha) = \frac{1}{\pi Q/2\gamma} \exp \left(- \frac{|d|^2}{Q/2\gamma} \right)$$

α may represent a single mode of a chaotic field with a Lorentz spectrum

Single mode laser

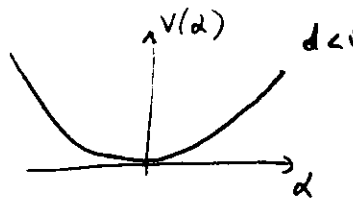
$$\ddot{\alpha} + (\gamma - G)\dot{\alpha} = \Gamma(t)$$

G : gain

$$G = g_0 - \beta |\alpha|^2 \quad \text{saturable gain} \rightarrow \text{nonlinearity}$$

$$\ddot{\alpha} - \beta(d - |\alpha|^2)\alpha = \Gamma(t) \quad d = (g_0 - \gamma)/\beta$$

(13)



$$\ddot{\alpha} + \frac{\partial V}{\partial \alpha} = \Gamma(t)$$

$$\text{F.P. Eq.} \quad \frac{\partial W_c}{\partial t} + \beta \operatorname{div}_\alpha \left[(d - |\alpha|^2) \alpha W_c \right] = \frac{Q}{4} \nabla_\alpha^2 W_c$$

$$\text{Put } \alpha = r e^{i\varphi}$$

$$\frac{\partial W_c}{\partial t} + \frac{\beta}{r} \frac{\partial}{\partial r} \left[(d - r^2) r W_c \right] = \frac{Q}{4} \left[\frac{1}{r} \frac{\partial}{\partial r} \left(r \frac{\partial W_c}{\partial r} \right) + \frac{1}{r^2} \frac{\partial^2 W_c}{\partial r^2} \right]$$

Stationary solution

$$W(r, \varphi) = N \exp \left[- \frac{P}{Q} r^2 + \frac{2pd}{Q} r^2 \right]$$

Threshold $g_0 = \gamma \rightarrow d = 0$

$$\text{For below threshold } d < 0 : W = N \exp \left(- \frac{2p|d|r^2}{Q} \right)$$

Gaussian distribution with $\langle r^2 \rangle = Q/2p|d|$

For above threshold $d > 0$

$$W = N \exp \left[- \frac{4pd}{Q} (r - \sqrt{d})^2 \right]$$

Displaced Gaussian $\langle r^2 \rangle = d$

Correlation functions

$$\text{For below threshold } |G_1(\tau)| = \frac{Q}{2p|d|} e^{-2p|d|\tau} \quad \left. \begin{array}{l} \text{Gaussian} \\ \text{process} \end{array} \right\}$$

$$G_2(\tau) = \langle |\alpha|^2 \rangle + \left(\frac{Q}{2p|d|} \right)^2 e^{-4p|d|\tau}$$

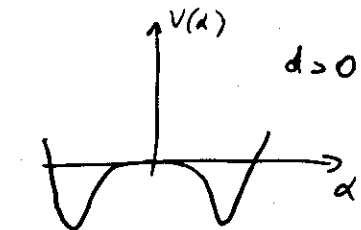
For above threshold

$$|G_1(\tau)| = d e^{-(Q/4d)\tau} + \frac{Q}{8pd} e^{-(2pd + Q/4d)\tau}$$

$$G_2(\tau) = \langle |\alpha|^2 \rangle + \frac{Q}{2p} e^{-2pd\tau}$$

Above threshold the main noise is phase difference noise

(14)



Measurement of ultrashort pulse duration by harmonic generation or multiphoton fluorescence

(15)

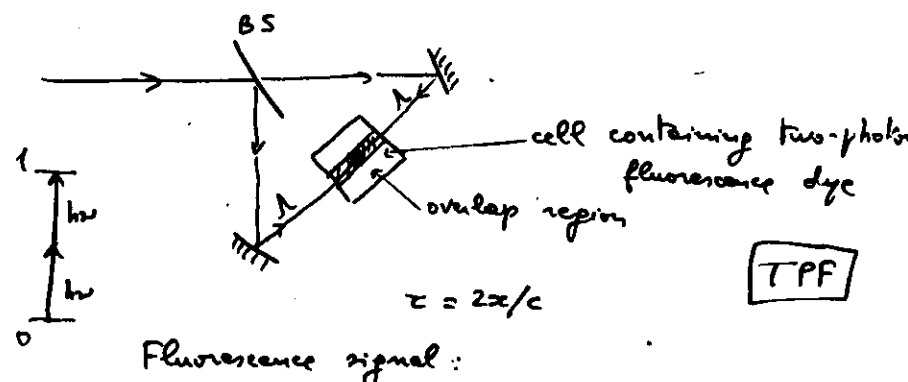
E_{SHG} is $\neq 0$ only if E_1 and E_2 are simultaneously present

(16)

$$I_{SH} = \kappa \int |E_1(t) E_2(t+\tau)|^2 dt \\ = \kappa \{ G_2(\tau) + \text{rapidly varying terms} \}$$

Commercial optical autocorrelator (only for a long pulse train, whereas TPF works with a single pulse)

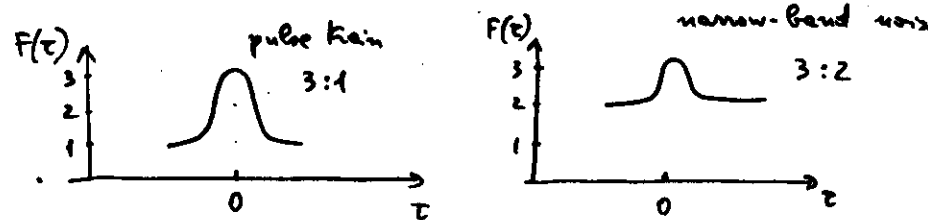
Translation stage: 2 μm per step
(12 fs = 12×10^{-15} s)



Fluorescence signal:

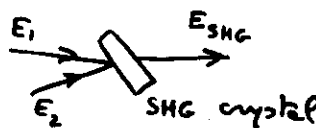
$$F(\tau) = \kappa \int |E_1(t) + E_2(t+\tau)|^4 dt = \\ = \kappa \{ G_2(0) + 2G_2(\tau) + \text{rapidly varying terms} \}$$

$$G_2(\tau) = \langle I(t) I(t+\tau) \rangle$$

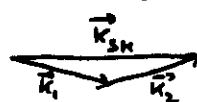


$$1 \text{ ps} \Rightarrow 0.3 \text{ nm}$$

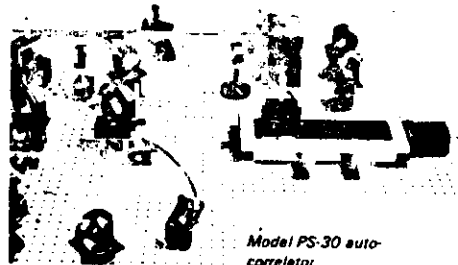
It is possible to obtain background-free measurement by exploiting second harmonic generation (SHG):



Pulse matching:



The optical arrangement of the Model PS-30 is shown schematically in the figure below and part of the optical layout shown in the photograph.



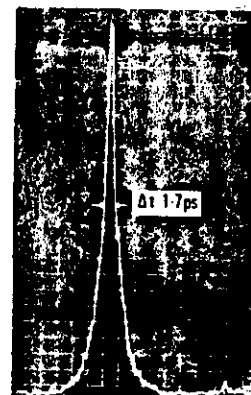
Model PS-30 auto-correlator

The laser pulse train is divided into two beams by means of a partially-reflecting beam-splitter. The two replica pulses traverse different paths in an interferometer before being recombined in a non-linear second harmonic generating (SHG) crystal. The path length of one arm can be varied by driving the translation stage with a stepping motor controlled by a microcomputer. If the two beams enter the same region of the SHG crystal, frequency doubling will be observed for any length of the variable arm. However, when the two pulses are coincident in time and space, the second harmonic signal with zero background will be observed. Signal to noise ratios can be enhanced considerably by repetitive scanning and a representative pulse profile is shown in the photograph.

The optical system is carefully designed to eliminate feedback into the laser. The translation stage has a movement of 2 μm per step, equivalent to 12 fs in this configuration. All optical components are mounted on high precision mounts (resolution 0.2 arc sec) and supplied with magnetic mounts. These mounts

give infinitely variable positioning capability and minimise the set up time. Once aligned on a suitable table, the system does not require realignment for long periods of time.

It is necessary to use some form of optical table to provide a common structure to which the laser and optical components of the Optical Auto-correlator can be secured. The performance of such a table can be measured in terms of how well the optical components and laser retain their relative positions in the presence of disturbing forces (such as floor or ground



Second harmonic auto-correlation trace of sync-pumped dye laser pulse at 590 nm

motion) or unfavourable ambient conditions, including thermal inputs to the table by convection, conduction or radiation. Although the photon counting equipment may be mounted on a steel-topped wooden table, we use and recommend NRC honeycomb tables for the Auto-correlator and the MCA and Spectrometer. These special tables (usually 3.0 x 1.6 m) have excellent thermal stability and use internal damping systems to reduce the resonant response of the tops and to ensure that the table top will remain rigid for both static and dynamic

